POAC'25
St. John's, Newfoundland and Labrador, Canada

Proceedings of the 28th International Conference on Port and Ocean Engineering under Arctic Conditions
Jul 13-17, 2025
St. John's, Newfoundland and Labrador
Canada

The prediction of hull strain for a polar vessel from structural vibration with transmissibility-based transfer function models

Gerhard Durandt[1], Anriëtte Bekker[1]
[1]Department of Mechanical and Mechatronic Engineering, Faculty of Engineering, Stellenbosch University, Stellenbosch, South Africa, 7600

ABSTRACT

The virtual sensor is a digital twin use case with the potential to inform operational and tactical decision-making towards increased vessel safety, passenger comfort and sustainable operations. A polar vessel, instrumented with accelerometers and strain gauges, suffers accelerated fatigue due to the resonant excitation of the hull structure from wave slamming. A transmissibility-based transfer function matrix is computed using the Operational Transfer Path Analysis method. Structural acceleration data from ice operations in the Antarctic marginal ice zone (MIZ) serve as the input degrees of freedom. The structural strain near midship is predicted from the global structural vibration and validated.

This work is the first step towards enabling virtual strain measurement on a vessel that suffers a high probability of impulsive slamming loads, stemming from the hydrodynamic interaction between the ocean and ice rated hull geometry. The transmissibility relationship unlocks the potential to estimate the midship strain response in the absence of a strain sensor. As a result, the strain history of a vessel could be predicted based on historical structural accelerometer data. Virtual strain enables the progression of a structural digital twin by including the accumulated high-frequency fatigue from ice-induced vibration into an analysis of actually accrued hull fatigue. Consequently, this virtual sensor could provide ship owners with valuable information and tools to manage accumulated high-frequency hull fatigue effectively and inform decision-making to increase remaining useful life.

KEY WORDS: Operational Transfer Path Analysis; Virtual Sensor; Structural Digital Twin; Polar vessel

INTRODUCTION

Digital twin technology promises to propel data-based decision-making for maritime operations and vessel design into a new frontier. A digital twin is a virtual representation of a physical asset that conveys information regarding the asset operation, performance, health and environment within a sufficient time horizon to deliver decision support (Erikstad, 2017; Fonseca & Gaspar, 2021). The advantage a digital twin presents to industry is enabled by data-driven insights for operational decision support. This can manifest in several applications, including structural health monitoring and predictive maintenance (Madusanka, et al., 2023).

Narrowing the focus of the digital twin to the hull structure of polar vessel may yield insight into the operational loading conditions and stress peaks over time. Consequently, it raises

questions such as estimating accumulated structural fatigue and its effect on the remaining useful life of a vessel – factors that are important for owners and investors from the *return on investment* perspective. Although direct strain measurement may be the ideal method to monitor stress cycles, the installation and maintenance of strain gauges require significant effort in the long term. Strain gauge installation and maintenance is a labour-intensive process and sensitive to installation errors (Hoffmann, 1989). The installation of strain sensors require adhesion at a precise orientation potentially performed in areas which do not support the ergonomics of test technicians. This is especially true for retrofit sensor installations.

In contrast, accelerometers are much lower effort to install especially with regards to sensor adhesion and orientation. Furthermore, acceleration responses at higher frequencies have higher (more measurable) response amplitudes if compared to deflection. Acceleration measurements potentially offer a greater signal-to-noise ratio and enhanced measurement resolution. The main disadvantage is that relationship between structural strain and structural acceleration is more obscure.

Virtual measurement is a methodology under the digital twin umbrella that may provide a means to address this problem. The operational use of hull measurements in combination with digital models enables virtual strain sensing to predict key performance indicators when direct measurement is prohibitively difficult or expensive to implement. In essence, a virtual sensor utilizes data from physical sensors in conjunction with some form of system model to predict a parameter of interest (Tarpø, 2020).

In the case of a structural digital twin the direct measurement of the hull strain over the life cycle of a vessel, or retrofitting strain sensors on an existing vessel, may be difficult and expensive to implement in the long term. Alternatively, virtual sensors can transform the measurements from a network of accelerometers located all over the structure into a predicted strain response at another location without the long-term installation and maintenance of strain sensors. Accelerometers are installed with relatively less effort and the strain is estimated with a computational model.

The aim of this paper is to demonstrate the transmissibility relationship between structural acceleration and strain and how it can be utilized as a virtual strain sensor for a ship with an ice-going hull design during ice navigation. The methodology for the transmissibility-based model is grounded in Transfer Path Analysis (TPA), which has the capability of synthesizing a transfer function model from operational measurements for a set of input and output degrees of freedom (DOF) (van der Seijs, et al., 2015). TPA is mainly adopted by the automotive industry to address noise, vibration and harshness problems in the frequency domain (van der Seijs, et al., 2015; de Klerk & Ossipov, 2010). Therefore, literature on the application of TPA in other sectors, such as shipping, is limited. The contribution from this study is the novel application of TPA to facilitate virtual strain sensing in the maritime context.

This work presents a case study on a Polar Supply and Research Vessel (PSRV). First, the full-scale measurement infrastructure onboard the PSRV is presented. Next, a brief theoretical overview of TPA and its mathematical formulation is discussed. The model is applied to operational data recorded during ice navigation on a scientific voyage to the Antarctic marginal ice zone (MIZ). Finally, the results are validated against a secondary data set and discussed.

METHODOLOGY

Measurement infrastructure

The hull monitoring system consists of a network of accelerometers attached throughout the

hull structure of the PSRV. The global rigid body and resonant vibration modes are measured while at sea and during ice-navigation. The vessel regularly sails between Cape Town and Antarctica and serves as a unique case study for research in system identification and the application of operational modal analysis (OMA) (van Zijl, et al., 2021), human exposure to full-body vibration (Omer & Bekker, 2018) and hull fatigue (Pferdekämper & Bekker, 2024).

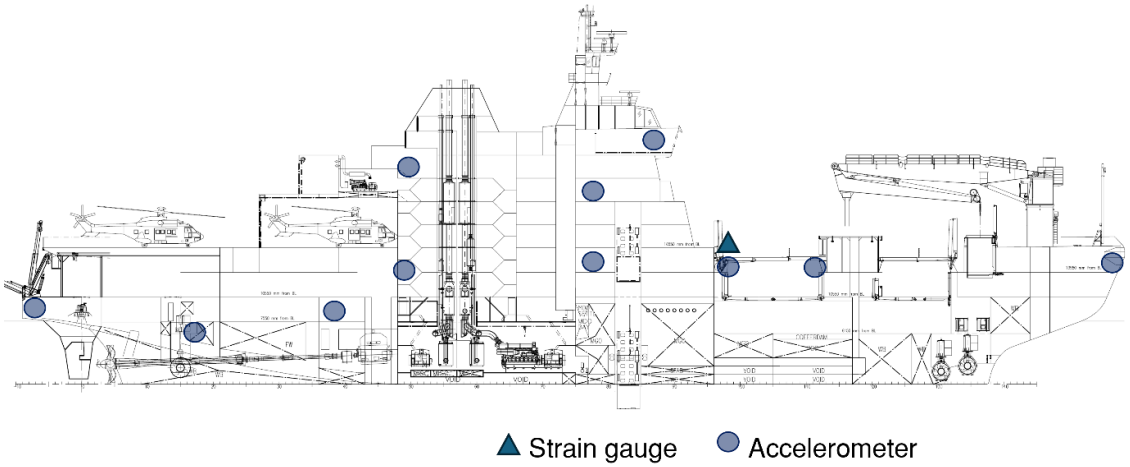

Figure 1: Sensor locations on the PSRV. Adapted from STX Finland (STX Finland, 2012).

A diagram showing the measurement locations is presented in Figure 1. A network of 26 integrated electronic piezo-electric (IEPE) accelerometers are placed throughout the structure to measure the global vibration response. Strain gauge sensors are installed near midship at frame 98 on both the port and starboard sides. This location is selected due to the significant change in the transverse cross-section where it is believed that high bending stresses are present. This claim is substantiated in literature where visible cracks were reported near frame 98 (Pferdekämper & Bekker, 2024). Data from the strain sensors are utilized in two ways. Firstly, it is a critical initial parameter to synthesize the virtual sensor. Secondly, it serves as a verification of the virtual sensor's performance.

The ship has a Polar Class 5 ice class notation, an overall length between perpendiculars of 121 m and is powered by two 4 500 kW electric motors. This enables the vessel to pass through 1 m thick ice at a speed of 5 knots (SANAP, n.d.). All measurement channels are sampled at 2048 Hz.

Theoretical overview of TPA

TPA is an experimental technique typically associated with noise, vibration and harshness problems in the automotive industry. Various TPA methodologies are reported in literature and are normally grouped into three categories, i.e. classical TPA, component-based TPA, and transmissibility-based TPA (van der Seijs, et al., 2015).

Classical and component-based TPA relies on the measured frequency response functions (FRF) of a structure or component to synthesize a model between a set of input and output DOF. Explicit knowledge of the input forces yields comprehensive information about the dynamic behaviour of the structure (van der Seijs, et al., 2015). The input forces are typically measured with specialized equipment such as modal shakers or modal hammers. Despite this, on the scale of a typical icebreaking ship it is generally not feasible to apply controlled forces of adequate magnitude to perform a reliable experimental modal analysis (EMA) to measure

the FRF's. Similarly, in the general case of ice navigation, knowledge of the force interaction between the hull structure and ice is complex to describe, with modern methods relying heavily on simulation (Tuhkuri & Polojärvi, 2018; Paavilainen & Tuhkuri, 2013; Gong, et al., 2023).

Transmissibility-based TPA, otherwise referred to as Operational Transfer Path Analysis (OTPA), differs from the former two methods. OTPA aims to determine the path relationship between a set of input and output channels without the determination of FRF's. Instead, the path relationships are described by a transfer function, known as a transmissibility matrix, between the measured input and output DOF (van der Seijs, et al., 2015; de Klerk & Ossipov, 2010). This makes OTPA an appropriate technique to apply in an operational environment by essentially avoiding the direct force measurement of the complex ice-structure interaction. Specifically, the computed transmissibility matrix serves as the virtual sensor that relates the measured structural acceleration response to a predicted strain response at a specific location.

OTPA formulation with singular value decomposition

The OTPA algorithm is a signal processing method that utilizes singular value decomposition (SVD) and cross-talk cancellation (CTC) to find a linearized transfer function matrix between a set of input and output parameters (de Klerk & Ossipov, 2010). Consider a linear model of a multiple DOF system. In the frequency domain, the system can be described as

$$\boldsymbol{H}(j\omega)\boldsymbol{x}(j\omega) = \boldsymbol{y}(j\omega) \tag{1}$$

where the output vector, $\boldsymbol{y}(j\omega)$, is modelled as the product of the transfer function matrix, $\boldsymbol{H}(j\omega)$, and the input vector, $\boldsymbol{x}(j\omega)$. The size of the input and output vectors, $\boldsymbol{x}$ and $\boldsymbol{y}$, are determined by the number of measurement channels included in the measurement. The measurement channels are analogous to the number of input and output DOF.

The input and output vectors can represent any realistic physical quantity related to the DOF of the model, such as motions, $\boldsymbol{u}(j\omega)$, forces, $\boldsymbol{f}(j\omega)$, or strain, $\boldsymbol{\varepsilon}(j\omega)$. Note the dependency on frequency with the symbols $j\omega$ and the use of complex numbers. This requires that time-based measurements are transformed to the frequency domain with the Fourier transform before constructing the associated input and output vectors. The symbols $j\omega$ are omitted from this point for clarity. Now, the input and output vectors are constructed as

$$\boldsymbol{x} = \begin{bmatrix} \boldsymbol{u}_x \\ \boldsymbol{f}_x \\ \boldsymbol{\varepsilon}_x \end{bmatrix}; \qquad \boldsymbol{y} = \begin{bmatrix} \boldsymbol{u}_y \\ \boldsymbol{f}_y \\ \boldsymbol{\varepsilon}_y \end{bmatrix} \tag{2}$$

It is up to the engineer to define the input and output vectors from the measured data. In the specific case presented in this paper, the input vector is constructed from measured acceleration and output vectors from the strain measurements at frame 98. The input and output vectors are expanded as shown in Equation (3). The indices, m and n, refer to the number of channels associated with the input or output measurements respectively.

$$\boldsymbol{u}_x = \left[u_x^{(1)}, \dots, u_x^{(m)}\right]^T; \qquad \boldsymbol{\varepsilon}_y = \left[\varepsilon_y^{(1)}, \dots, \varepsilon_y^{(n)}\right]^T \tag{3}$$

From the construction of Equation (1), the elements of the transfer function matrix $\boldsymbol{H}$ takes the form (de Klerk & Ossipov, 2010)

$$H_{ij} = \left.\frac{y_i}{x_j}\right|_{x_k=0} \quad ; \quad k \neq j \tag{4}$$

In an ideal scenario, the element-wise determination of $\boldsymbol{H}$ is normally performed using EMA where an external force is applied, x_j, at a single DOF while the forces at all other DOF are suppressed. In the laboratory, this force can be generated with a shaker or modal hammer. However, this is an impossible experimental setup in the operational environment of an icebreaking vessel where the input vector, $\boldsymbol{x}$, consists of the global vibration response of the structure. With OTPA this drawback is overcome by attempting to measure the transfer function matrix elements all at once (de Klerk & Ossipov, 2010). First, the transpose of Equation (1) is taken and expended element-wise as

$$\left[x^{(1)}, \dots, x^{(m)}\right] \begin{bmatrix} H_{11} & \dots & H_{1n} \\ \vdots & \ddots & \vdots \\ H_{m1} & \dots & H_{mn} \end{bmatrix} = \left[y^{(1)}, \dots, y^{(n)}\right] \tag{5}$$

Here, the number of input and output channels are denoted by the parameters m and n respectively. This operation on its own does not allow the direct computation of the transfer function matrix elements. Instead, Equation (5) is expanded to include several measurement blocks with no overlapping content. For example, in the maritime context, a 30-minute measurement can be cut into a number of smaller blocks. The random and impulsive nature of ice-structure interaction means that the time-domain structural response will be different for each measurement block. Assuming the relationship between the input and output parameters remains linear throughout the whole measurement, then the transfer function described in Equation (5) should be true for each measurement block r as

$$\begin{bmatrix} x_1^{(1)} & \dots & x_1^{(m)} \\ \vdots & \ddots & \vdots \\ x_r^{(1)} & \dots & x_r^{(m)} \end{bmatrix} \begin{bmatrix} H_{11} & \dots & H_{1n} \\ \vdots & \ddots & \vdots \\ H_{m1} & \dots & H_{mn} \end{bmatrix} = \begin{bmatrix} y_1^{(1)} & \dots & y_1^{(n)} \\ \vdots & \ddots & \vdots \\ y_r^{(1)} & \dots & y_r^{(n)} \end{bmatrix} - \mu \tag{6}$$

With this formulation the model requires the elements of the transfer function to be linearly independent and makes Equation (6) a solvable least-squares optimization problem. The additional residual μ contains the content that cannot be modelled by the selected input DOF. Next, a compact form of Equation (5) is presented as

$$\boldsymbol{XH} + \mu = \boldsymbol{Y} \tag{7}$$

Equation (7) is solved for each frequency line in the FFT spectrum. This is accomplished by pre-multiplying with $\boldsymbol{X}^T$ and ensuring that the residual vector is in the null space of the input DOF, meaning that $\boldsymbol{X}^T\mu = \boldsymbol{0}$. This results in the transfer function taking the form of

$$\boldsymbol{H} = (\boldsymbol{X}^T\boldsymbol{X})^{-1}\boldsymbol{X}^T\boldsymbol{Y} = \boldsymbol{X}^+\boldsymbol{Y} \tag{8}$$

The next step entails the expression of the input vector $\boldsymbol{X}$ in terms of a SVD to prevent poor estimates and minimise the effects of measurement noise on the prediction.

$$\boldsymbol{X} = \boldsymbol{U}\boldsymbol{\Sigma}\boldsymbol{V}^T \tag{9}$$

Here, $\boldsymbol{U}$ is a $r \times r$ unitary matrix, $\boldsymbol{\Sigma}$ is a $r \times m$ matrix with positive numbers on the diagonal and zeros off the diagonal. $\boldsymbol{V}^T$ is the conjugate transpose of $\boldsymbol{V}$ which is a $m \times m$ unitary matrix. This allows for the expression of the pseudo-inverse matrix $\boldsymbol{X}^+$ as

$$\boldsymbol{X}^+ = \boldsymbol{V}\boldsymbol{\Sigma}^{-1}\boldsymbol{U}^T \tag{10}$$

Finally, by substituting Equation (10) into Equation (8) yields the transfer function matrix $\widetilde{\boldsymbol{H}}$ as

$$\widetilde{\boldsymbol{H}} = \boldsymbol{V}\boldsymbol{\Sigma}^{-1}\boldsymbol{U}^T\boldsymbol{Y} \tag{11}$$

Consequently, with the newly obtained transfer function matrix it is possible to predict the output DOF with new a new input data set.

$$\widehat{\boldsymbol{Y}} = \boldsymbol{X}_{new}\widetilde{\boldsymbol{H}} \tag{12}$$

In the context of this paper, the predicted output vector is the strain response, while the input vector is populated with acceleration channels measured for the hull structure.

RESULTS

Scientific voyage, ice conditions and datasets

Measurements were conducted during a scientific voyage in the Southern Ocean between Cape Town and the Antarctic MIZ during the winter of 2022. The route of the ship is shown in Figure 2 with the ship encountering and navigating sea ice from latitudes 58°S and higher for a period of six consecutive days.

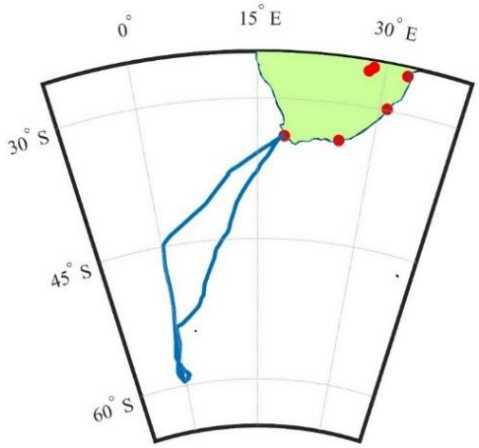

Figure 2: Route of the PSRV from Cape Town to the Antarctic MIZ (11-31 July 2022).

The ice conditions that were encountered consisted mostly of newly formed level sea ice and fields of pancake ice. Researchers onboard the vessel conducted visual ice observations from the bridge during all hours while the ship was in motion. Estimates of the ice concentration, floe thickness and floe diameter were recorded every minute in accordance with the methods described in (Bekker, et al., 2017). Table 1 lists the ice conditions associated with three datasets used to compute and validate the model. The transfer function model was synthesized with the training set and validated with validation set 1 and validation set 2. Validation set 1 was measured during similar operational conditions as the training set, while validation set 2 was acquired at a higher speed and with thicker ice. The length of all three data sets spanned a period of 30-minutes.

The primary dataset was used to compute the transfer function matrix, as described by Equation (11). The input vector, $\boldsymbol{X}$, was populated with acceleration data from the 26 input channels from the training set. Likewise, the output vector, $\boldsymbol{Y}$, was constructed from the two strain gauge channels located on the port and starboards sides at frame 98. Therefore, the transfer function matrix, $\widetilde{\boldsymbol{H}}$, was computed for each frequency line as described in Equation (11). Similarly, a new input vector, $\boldsymbol{X}_{new}$, was constructed for each of the two validation sets. The associated predicted strain, $\widehat{\boldsymbol{Y}}$, was then computed with Equation (12).

After synthesizing the transfer function matrix, $\widetilde{\boldsymbol{H}}$, it essentially becomes a collection of frequency dependent transfer functions relating each input channel to each of the output channels. In this case, $\widetilde{\boldsymbol{H}}$ contains 26×2 transfer functions ($m \times n$). The frequency plot of the transfer function between an accelerometer located in the bow and the port side strain gauge is shown in Figure 3. It was assumed that the impulsive loads from ice impacts produces a broadband excitation. Therefore, the number of measurement blocks for the OTPA computation was set to $r = 1$.

Table 1: Ice conditions from visual observations for the training and validation data sets over a 30-minute window.

Dataset	*Date*	*Time (UTC)*	*Ship speed (kn)*	*Ice concentration (%)*	*Floe thickness (cm)*	*Estimated Floe diameter (m)*
Training set	20/07/2022	20:00-20:30	6.2	87.2	29.7	2497
Validation set 1	20/07/2022	20:30–21:00	5.01	88.7	31.3	3491
Validation set 2	22/07/2022	08:40-09:10	13.1	91	37.7	81.6

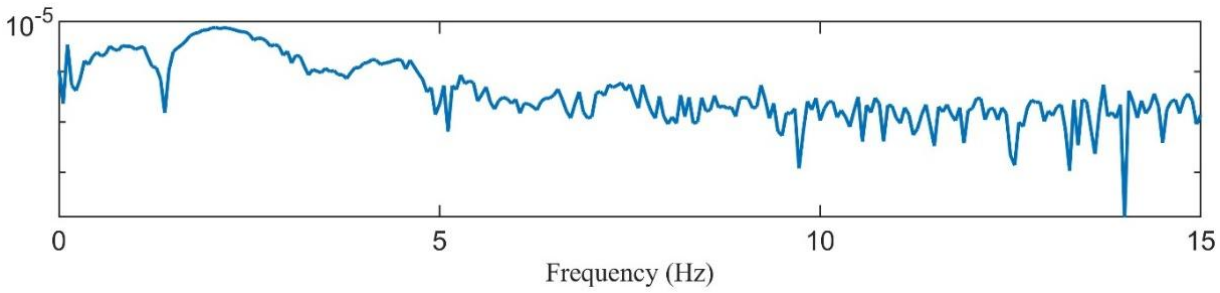

Figure 3: Frequency response of the transfer function relation between a bow accelerometer (input) and the port side strain gauge (output).

Validation set 1

In Figure 4 the set of graphs with the time and frequency response of the predicted strain for validation set 1 is presented. The ice conditions for validation set 1 was similar to the original training data and evaluates the model's performance under similar operating conditions. Figure 4 (a) shows the raw 30-minute strain prediction from the transfer function matrix with no additional signal processing. A slight bias error is observed between the predicted and measured signals. The lower limit of the frequency range for the installed accelerometers is 0.5 Hz (PCB Piezotronics, 2009). Therefore, a high-pass filter was applied to remove frequency content below 0.5 Hz. As a result, the bias error was removed as shown in Figure 4 (b) and (c). The frequency response, Figure 4 (d), was calculated with the FFT algorithm (0% overlap, uniform window, block size = 921 600). It is observed that the frequency content of the predicted strain matches the measured peak values associated with the structure's natural frequencies.

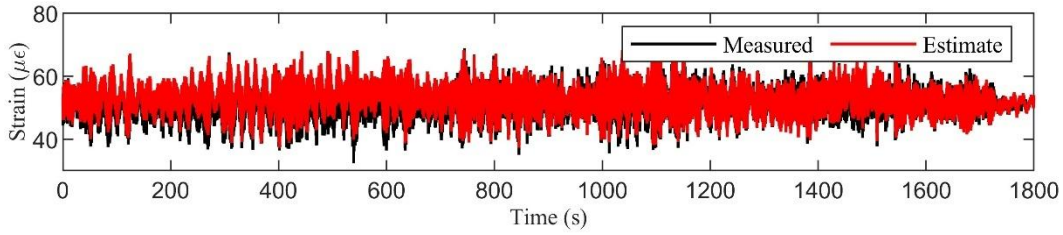

(a)

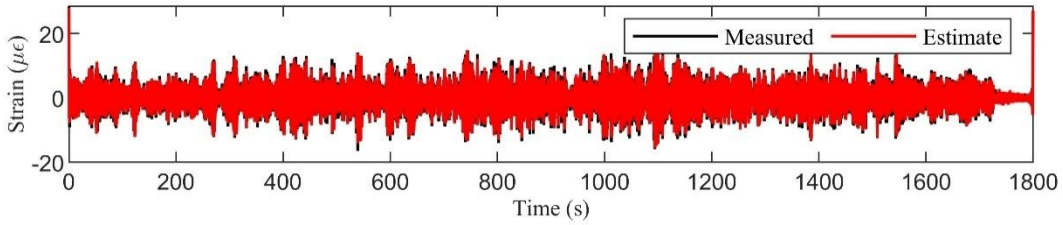

(b)

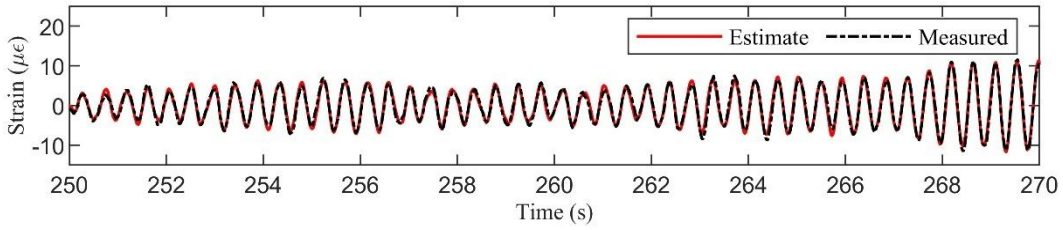

(c)

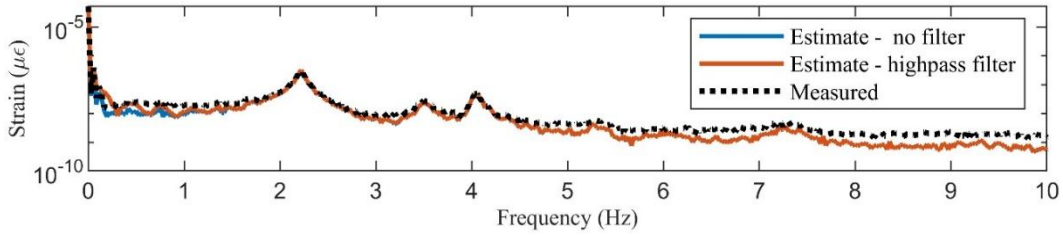

(d)

Figure 4: Validation set 1: time response with no filter (a), high-pass filter (b), close-up representation with high-pass filter (c) and FFT response of predicted strain (d) [0% overlap, uniform window, block size = 921 600].

Validation set 2

In Figure 5 the set of graphs with the time and frequency response of the predicted strain for validation set 2 is presented. The ice conditions for validation set 2 were different to the original training data in terms of the vessel's speed, ice thickness and floe size, which evaluates the model's performance under a change in operating conditions. Figure 5 (a) shows the raw 30-minute strain prediction from the transfer function matrix with no additional signal processing applied. A larger bias error is observed between the predicted and measured signals compared to the initial estimates from validations set 1.

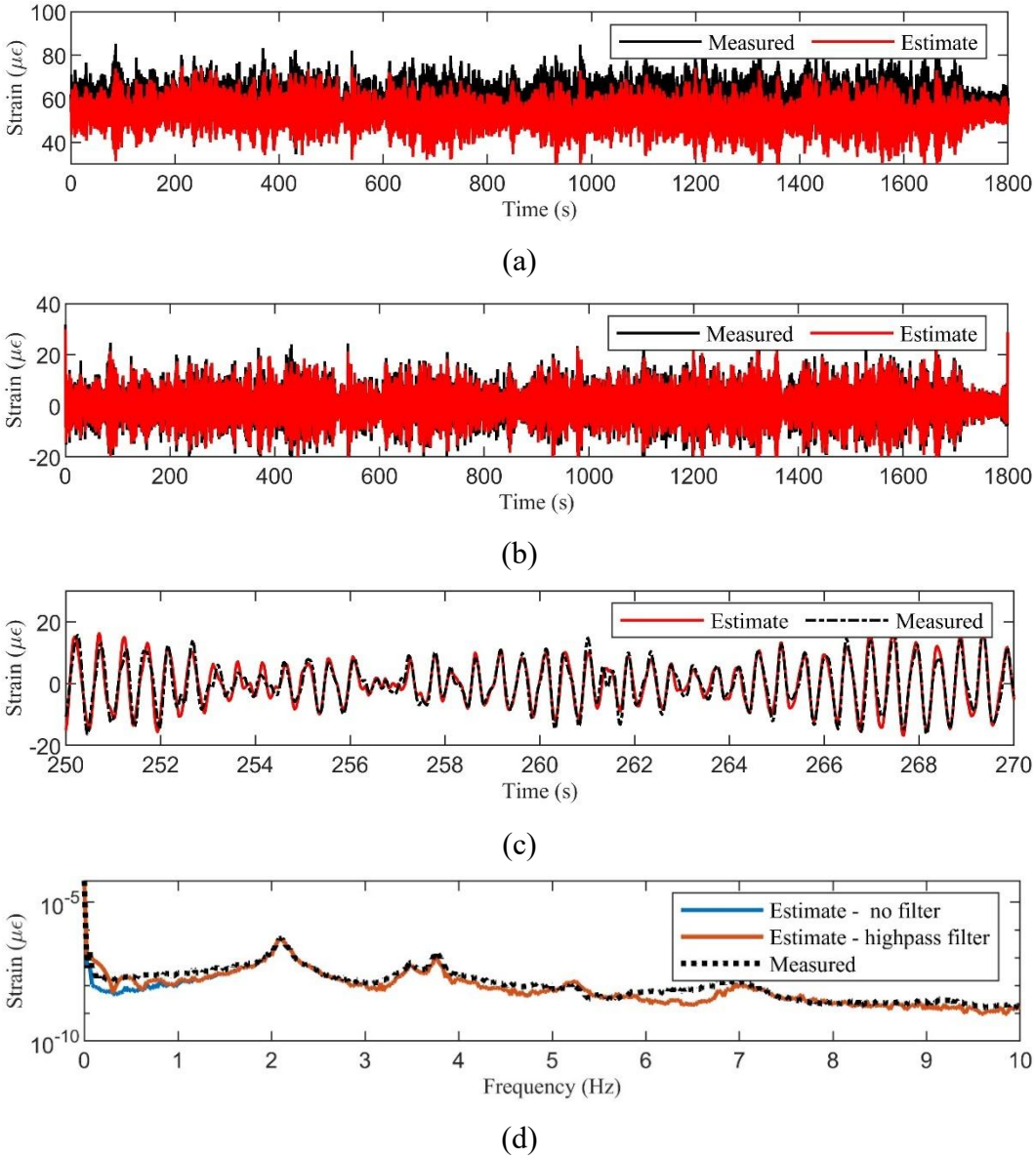

Figure 5: Validation set 2: time response with no filter (a), high-pass filter (b), close-up representation with high-pass filter (c) and FFT response of predicted strain (d) [0% overlap, uniform window, block size = 921 600].

Again, a high-pass filter was applied to remove frequency content below 0.5 Hz. Similar as before, the bias error was removed as shown in Figure 5 (b) and (c). The frequency response, Figure 5 (d), was again calculated with the FFT algorithm (0% overlap, uniform window, block size = 921 600). It is observed that the frequency content of the predicted strain matches the measured peak values associated with the structure's natural frequencies.

The quality and fit of the predictions were evaluated with the normalized root mean square error (NRMSE) metric. The NRMSE compares the accuracy of the predictive model to the observed values, normalized by the range of the observed data. Table 2 lists the NRMSE of both validation sets. The smaller error for validation set 1 was expected due to the similar operational conditions to the training set. Furthermore, a reduced NRMSE is observed after the high-pass filter was applied.

Table 2: NRMSE for validation set 1 and 2 before and after filtering

Dataset	$NRMSE_{no\ filter}\ (\mu\varepsilon)$	$NRMSE_{high\ pass\ filter}\ (\mu\varepsilon)$
Validation set 1	5.87	2.07
Validation set 2	10.28	3.11

DISCUSSION

The comparisons between the estimated and predicted strain in Figure 4 and Figure 5 illustrate that the transmissibility-based transfer function model has potential. Prior to any additional signal processing, the model predicted the strain response with reasonable accuracy for both validation data sets. In addition, it was accordingly expected, and ultimately shown in the FFT, that the transfer function model accurately predicted the measured natural frequencies associated with the peak values of the FFT.

Interestingly, the transfer function model initially produces a bias error when compared to the measured strain. This suggests that the model may lack low frequency content. In general, ocean waves that propagate through ice fields decrease in amplitude due to the scattering and dissipation of the wave energy (Squire, 2018), which may be a reason for the lack of low frequency excitation. Equally important, the unknown loading condition of the vessel and the sensitivity of the IEPE accelerometers at low frequencies may play an additional role. Further investigation is required to pinpoint to cause of the bias error.

The result produced a filtered strain prediction that closely correlated to the filtered measured strain for both data sets. This was highlighted by the low NMRSE in Table 2. Since the ice conditions and speed of the PSRV was different between the validation data sets suggests that the transfer function model remain somewhat constant between the two operating conditions. However, this assumption remains to be tested in more extreme conditions. Further validation is required for operations in general open water, or in established first year or multi-year ice fields.

In conclusion, the value of the OTPA method is associated with the reconstruction of the strain response from the acceleration response alone. Once the transfer function matrix, $\widetilde{\boldsymbol{H}}$, is synthesized then the need for long-term dynamic strain measurement theoretically becomes less important – assuming the model remains constant over time and over a range of operational conditions. Nonetheless, despite the modelling potential illustrated in this paper, the methodology still requires further research and validation.

CONCLUSION

A novel virtual sensor methodology based on OTPA was presented with the aim of developing modelling strategies to enable a structural digital twin for an ice rated vessel. An overview of OTPA and the formulation of the transmissibility-based transfer function model was discussed. Next, operational data from a PSRV during ice navigation in the Antarctic MIZ was employed to synthesize a transfer function matrix. This matrix serves as the model that relates the structural acceleration (input) to a predicted strain (output) response.

A validation study was performed to evaluate the performance of the transfer function model in two operational conditions during ice navigation. The initial strain prediction showed a bias error, which was subsequently removed with a high-pass filter. Consequently, the model accurately predicted the dynamic strain with low NRMSE values.

Further investigation into the performance of the model in extreme operational conditions, involving open water passage, and navigation in established first year or multi-year ice fields, are required. Nonetheless, the OTPA methodology shows modelling potential and could be utilized as a virtual strain sensor.

ACKNOWLEDGEMENTS

National Research Foundation (NRF) towards this research, through the South African National Antarctic Programme with Grant No. SANAP230511104945, and the DSI/SAIMI SARChI Chair for Naval Architecture and Design (RCNAD240703239108), is hereby acknowledged. Opinions expressed and conclusions arrived at are those of the authors and are not necessarily to be attributed to the NRF.

REFERENCES

Bekker, A., Soal, K. & McMahon, K., 2017. Whole-body vibration exposure on board a polar supply and research vessel in open water and in ice. *Cold Regions Science and Technology,* Volume 141, pp. 188-200.

de Klerk, D. & Ossipov, A., 2010. Operational transfer path analysis: Theory, guidelines and tire noise application. *Mechanical Systems and Signal Processing,* 24(7), pp. 1950-1962.

Erikstad, S. O., 2017. *Merging physics, big data analytics and simulation for the next-generation digital twins.* Hamburg, Germany, s.n., pp. 141-151.

Fonseca, Í. A. & Gaspar, H. M., 2021. Challenges when creating a cohesive digital twin ship: a data modelling perspective. *Ship Technology Research,* Volume 68, pp. 70-83.

Gong, H., Polojärvi, A. & Tuhkuri, J., 2023. *Velocity field and force distribution in an unconsolidated ice ridge penetrated by a ship.* Glasgow, United Kingdom, International Conference on Port and Ocean Engineering under Arctic Conditions (POAC).

Hoffmann, K., 1989. *An Introduction to Measurements using Strain Gages.* Darmstadt: Hottinger Baldwin Messtechnik GmbH.

Madusanka, N. S., Fan, Y., Yang, S. & Xiang, X., 2023. Digital twin in the maritime domain: A review and emerging trends. *Journal of Marine Science and Engineering,* Volume 11, p. 1021.

Omer, H. & Bekker, A., 2018. Human responses to wave slamming vibration on a polar supply and research vessel. *Applied Ergonomics,* Volume 67, pp. 71-82.

Paavilainen, J. & Tuhkuri, J., 2013. Pressure distributions and force chains during simulated ice rubbling against sloped structures. *Cold Regions Science and Technology,* Volume 85, pp. 157-174.

PCB Piezotronics, 2009. *333B32 datasheet.* Depew, New York: s.n.

Pferdekämper, K.-H. & Bekker, A., 2024. Investigation of vessel slamming and fatigue using a full-scale test sequence. *Applied Ocean Research,* Volume 144, p. 103883.

SANAP, n.d. *Vessels: Vessel Specification - S.A. Agulhas II.* [Online]
Available at: https://www.sanap.ac.za/explore/vessels
[Accessed 19 03 2025].

Squire, V. A., 2018. A fresh look at how ocean waves and sea ice interact. *Philosophical Transactions of the Royal Society A: Mathematical, Physical and Engineering Sciences,* Volume 376, p. 20170342.

STX Finland, 2012. *SA Agulhas II Technical Drawings.* s.l.:s.n.

Tarpø, M., 2020. *Stress estimation of offshore structures.* PhD Thesis: Aarhus University.

Tuhkuri, J. & Polojärvi, A., 2018. A review of discrete element simulation of ice-structure interaction. *Philosophical Transactions of the Royal Society A: Mathematical, Physical and Engineering Sciences,* Volume 376, p. 20170335.

van der Seijs, M. V., de Klerk, D. & Rixen, D. J., 2015. General framework for transfer path analysis: History, theory and classification of techniques. *Mechanical Systems and Signal Processing.*

van Zijl, C. et al., 2021. The use of operational modal analysis and mode tracking for insight into polar vessel operations. *Marine Structures,* Volume 79, p. 103043.